Contact Lens and Anterior Eye 41 (2018) 205–213

Contents lists available at ScienceDirect

Contact Lens and Anterior Eye

journal homepage: www.elsevier.com/locate/clae

An analysis of anterior scleral shape and its role in the design and fitting of scleral contact lenses

Markus Ritzmann[a,*], Patrick J. Caroline[b], Rainer Börret[c], Emily Korszen[d]

[a] Falco Linsen AG, Tägerwilen, Switzerland
[b] Pacific University, College of Optometry, Forest Grove, OR, USA
[c] Aalen University, Aalen, Germany
[d] Pacific University College of Optometry, Forest Grove, OR, USA

ARTICLE INFO

Keywords:
Anterior scleral shape
Scleral contact lenses
Visante OCT
Sagittal height
Corneo-scleral profile
Scleral angles
Scleral toricity
HVID
VVID
Corneal diameter
Limbal zone

ABSTRACT

Purpose: The purpose of this study was to evaluate the shape of the anterior sclera by measuring the sagittal height and corneoscleral transition angles in the four cardinal and four oblique segments of the eye.

Materials and methods: In this study, 78 normal eyes of 39 subjects were evaluated. The sagittal height, corneoscleral angle and scleral angle were measured at three chord lengths (10.0 mm, 12.8 mm and 15.0 mm) in all eight segments of the anterior eye using optical coherence tomography (Zeiss Visante AS-OCT). Scleral toricity was calculated for each eye, defined as the greatest sagittal height difference found between two perpendicular meridians.

Results: At a 12.8 mm chord length, the shape of the anterior eye was found to be nearly rotationally symmetric, and at a chord of 15.0 mm the shape became more asymmetric. The average sagittal heights of the eight segments at a 12.8 mm chord ranged from 2890 μm to 2940 μm; at a 15.0 mm chord they ranged from 3680 μm to 3790 μm. The average scleral angles at a 15.0 mm chord ranged from 35.17° to 38.82°. Significant differences between opposing segments were found in the sagittal height and scleral angle measurements at a chord of 15.0 mm (sagittal height $p \le 0.0021$; scleral angle $p \le 0.0105$). The nasal measurements revealed flatter scleral angles and concave corneoscleral transitions, whereas temporal scleral angles were steeper, with tangential or convex corneoscleral transitions.

Conclusion: These findings are important to consider when designing and fitting contact lenses that rest beyond the boundaries of the limbus, such as scleral lenses.

1. Introduction

The advent of videokeratoscopy in the early 1990's provided practitioners with new insights into the shape of the corneal surface across chords of 8.0–10.0 mm. More recently, through the use of composite corneal topography, it is possible to map the shape of the entire corneal surface from limbus to limbus. With the growing interest in contact lens designs that extend beyond the limbus, including modern scleral and soft contact lenses, researchers and clinicians have the need to look beyond the boundaries of the cornea to gain a greater understanding of anterior ocular shape and its impact on lens design [1–13].

The modern renaissance of scleral lenses has been made possible through the simultaneous development and merging of a number of technologies [14–18]. The availability of large diameter buttons of highly oxygen permeable materials, advances in computer controlled lathing techniques, and sophisticated lens design and fitting methods have all contributed to the success of this lens modality. Today scleral lenses serve as a primary tool in managing a wide range of conditions, including irregular astigmatism, ocular surface disease, and even normal refractive error [11,19–26].

Several studies have reported on the use of anterior segment OCT to describe the shape of the sclera by sagittal height [3,5–8], scleral radii [5–8,13,27] and scleral tangent angles [6,7,28]. A common finding was that the nasal sclera was flatter than the temporal in radii [6,7,13,27] and in terms of angle was smaller (lower angle) [5–7]. Additionally, authors have found consistent values of mean scleral sagittal depth at a chord of 15.0 mm, yet a strong disagreement exists among studies on scleral radii (Table 1). Additional biometric data of the anterior eye relevant to the design and fitting of contact lenses that rest beyond the limbus are displayed in Table 2.

Today, a number of questions related to scleral shape remain unanswered. For example, is the scleral surface spherical, toric, or

* Corresponding author.
E-mail address: scleral.lenses@gmail.com (M. Ritzmann).

http://dx.doi.org/10.1016/j.clae.2017.10.010
Received 21 June 2017; Received in revised form 27 September 2017; Accepted 6 October 2017

Table 1
Previous investigations of the anterior scleral shape by sagittal height (μm) and scleral radius (mm) imaged with the Visante OCT.

Ref.	n	n eyes	Age	Gender	Pathology	Sag 15 mm Horizontal (μm)	Sag 15 mm Vertical (μm)	Sag 15 mm MEAN (μm)	Radius Nasal (mm)	Radius Temporal (mm)
[5]	40	40	32	68% F	N/A	3740	N/A	3740	N/A	N/A
[6]	50	100	22.8 ± 5.0	70% F	normal	3740	3770	3760	45.0	25.3
[7]	204	204	34.9 ± 15.2	65% F	normal	3700	3750	3730	35.5	22.4
[8]	14	14	33 ± 7	79% F	normal	3710[a]	3700[b]	3710	N/A	N/A
	14	14	40 ± 14	36% F	keratoconus	3410[a]	3930[b]	3670	N/A	N/A
[13]	24	N/A	31.3 ± 6.5	50% F	normal	N/A	N/A	N/A	13.33[c]	12.32[c]
[27]	24	24	N/A	N/A	normal	N/A	N/A	N/A	13.68	11.73

[a] flat meridian.
[b] steep meridian.
[c] best-fit circle.

Table 2
Previous investigations of horizontal visible iris diameter (HVID), vertical visible iris diameter (VVID), and palpebral aperture.

Author	Ethnicity	n	n Eyes	Age	Gender	HVID (mm)	VVID (mm)	Palpebral Aperture (mm)
[29]	–	–	–	–	–	12.00	11.00	–
[30]	–	–	–	–	–	11.70	10.60	–
[31]	Caucasian	390	743	10–80	40% F	11.71	–	–
[6]	British Asian/Caucasian	50	100	23 ± 5	70% F	11.86	–	10.89
[32]	Nigerians	130	–	48 ± 17	41% F	11.39	10.51	–
[7]	British Asian/Caucasian	204	204	35 ± 15	65% F	11.70	–	10.20
[8]	–	14	14	33 ± 7	79% F	11.77	–	–

asymmetric? The present study was designed to gain a greater understanding of the shape of the anterior sclera. This knowledge will serve an important role in the development of future contact lens designs that rest beyond the limbus.

2. Materials and methods

This study was conducted in accordance with the tenets of the Declaration of Helsinki. In this cross-sectional study, the scleral contour of 78 normal eyes from 39 subjects was measured in eight primary meridians. Excluded from the study were subjects with inflammatory or ectatic conditions that may affect the elevation of the cornea, conjunctiva (pingueculae), episclera, and sclera. Also excluded were subjects with any history of ocular surgery. Daily soft contact lens wearers were requested to discontinue lens wear at least three days prior to data collection, and rigid gas permeable (RGP) and extended wearers (EW) at least ten days prior.

The Visante OCT (Carl Zeiss Meditec, Dublin, CA, USA) was used to measure the sagittal height of the anterior sclera at three different chord lengths of 10.0, 12.8, and 15.0 mm in all eight primary meridians at 0, 45, 90, 135, 180, 225, 270 and 315°. The 10.0 mm chord length was chosen as the largest chord for which the data could be compared to corneal topography measurements. The 12.8 mm chord was chosen to represent the beginning of the scleral tissue, 1.0 mm larger than the average HVID, and the 15.0 mm chord was chosen as the largest chord length that could be consistently measured with the OCT images. To provide additional information regarding the shape of the sclera, the corneoscleral angles were also measured at chords of 12.8 and 15.0 mm in all eight meridians.

The "Anterior Segment Quad" scan was used to image the four quadrants in cross-sections at 180, 45, 90 and 135°. This scan images the four quadrants simultaneously, allowing for accurate measurement and comparison between the eight segments (Fig. 1). To capture a full view of the anterior segment, the superior and inferior eyelids of the subjects were manually held open without applying any pressure to the globe.

Corneal topography was performed using the Medmont E300 corneal topographer (Medmont International Pty Ltd, Victoria, AUS), and each subject's objective refraction was assessed using the Grand Seiko WAM-5500 (Shigya Machinery Works Ltd, Fukuyama City, Hiroshima, Japan). The Haag Streit BQ900 photo slit lamp (Haag-Streit AG, Koeniz, Switzerland) and the MB-Ruler software (MB-Software solutions, Iffezheim, Germany) were used to analyze the palpebral aperture and horizontal and vertical visible iris diameters (Fig. 2).

The sagittal height and scleral angles were measured with the built-in caliper tool of the Visante Analysis Software. To set a reference line for the measurement calipers, landmarks on the anterior ocular surface were used, as opposed to internal landmarks such as the iris root or scleral spur. In each cross-sectional image, the external junction of the cornea and sclera was used to define the boundaries of the corneal diameter (Fig. 3). To locate the termination of the cornea on the anterior surface, the scleral spur was first identified, and a caliper was drawn from the scleral spur to the anterior surface, perpendicular to a line tangent to the surface. The corneal diameter was defined as the distance between the two opposing endpoints in each cross section. This method is similar to that used by ocular pathologists [30,33]. The distance between the opposing scleral spur locations was defined as the scleral spur to scleral spur distance. The anterior chamber tool placed at the two endpoints that mark the external corneal diameter was considered as the line of reference for all measurements at the three chord lengths of 10.0 mm 12.8 mm and 15.0 mm (Fig. 4). Sagittal height was measured as the distance (μm) from the ocular surface at each chord length to a line tangent to the corneal apex and parallel to the reference line described above. Therefore, the lower the sagittal height number, the greater the elevation of the tissue, and the higher the sagittal height number, the lesser the elevation. The corneal angle was measured using the anterior chamber angle-tool, and was formed by the 12.8 mm chord (parallel to the reference line) and a line along the corneal surface that connects the 10.0 mm and 12.8 mm chord endpoints. The scleral angle was similarly measured by placing the angle-tool at the junction of the 15.0 mm chord endpoint and a line connecting the 12.8 mm and 15.0 mm chords. The corneo scleral junction (CSJ) angle was measured as the external angle formed between the line connecting the 10.0 mm and 12.8 mm chords and the line connecting the 12.8 mm and 15.0 mm chords. The CSJ angle describes the transition from cornea to sclera as either concave (<180°), tangential (=180°) or convex (>180°). The

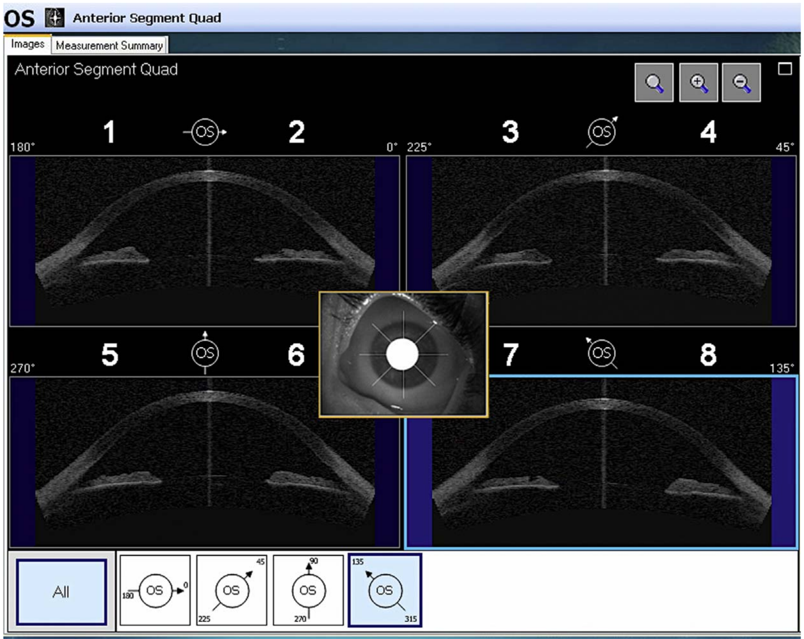

Fig. 1. Visante OCT Anterior Segment Quad Scan with four cross sections simultaneously scanned.

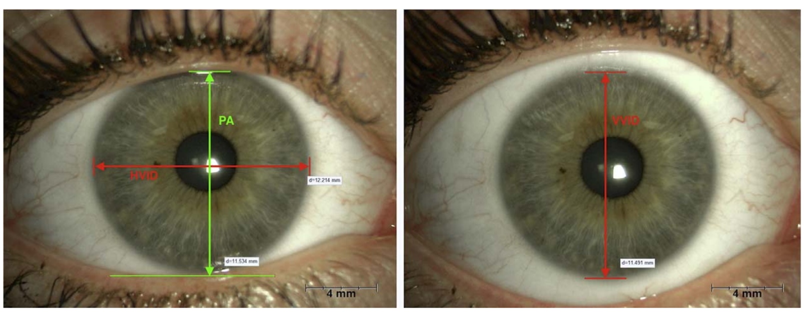

Fig. 2. HVID, VVID and PA measurements on Haag Streit slit lamp images using MB Ruler Software.

limbal zone was defined as the area between the corneal diameter and the visible iris diameter.

The study data was analyzed with the Prism V6.0 software (GraphPad Software, Inc., La Jolla, CA, USA). The Shapiro-Wilk's test was performed for every ocular variable to identify any deviations from the normal distribution, using the critical value of 0.05. For comparison of paired data, either the paired *t*-test or the Wilkoxon signed rank test was used and a significance criteria of $p < 0.05$ was applied. Data from right and left eyes were not combined in order to avoid altering the significance of the results [34].

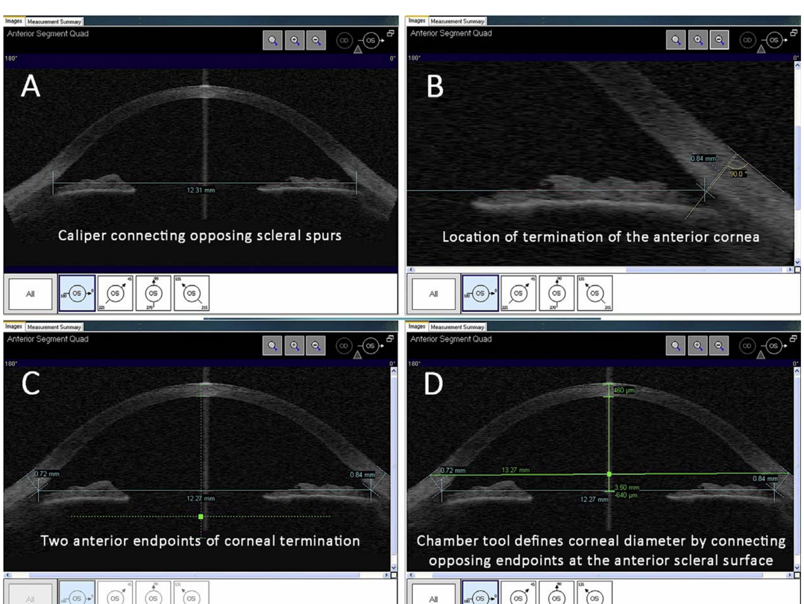

Fig. 3. Visante OCT image analysis: four steps were used to define the corneal diameter (CD).

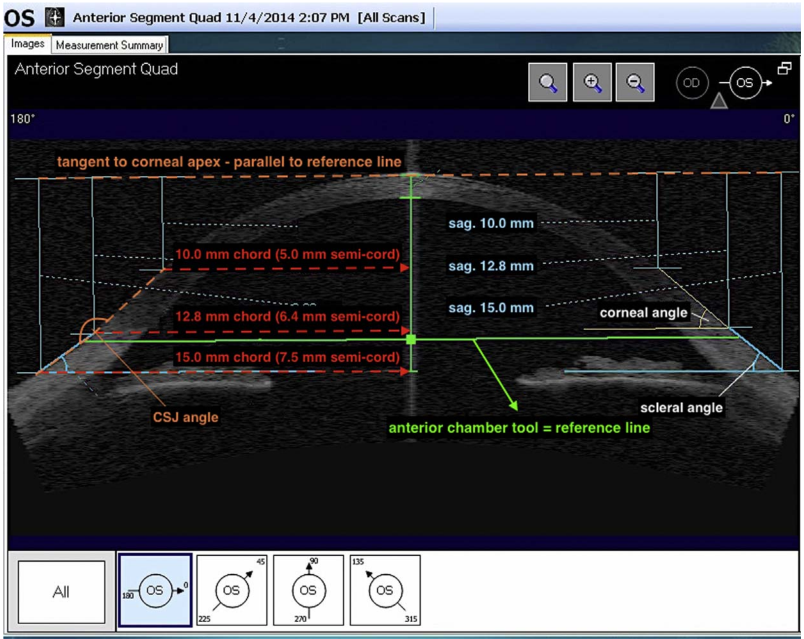

Fig. 4. Visante OCT image analysis showing scleral sagittal height and corneoscleral angle measurements in one cross section.

3. Results

Of the 39 qualified subjects, 29 were female (74%) and 10 were male (26%). The mean age was 25.4 ± 2.0 years; 37 subjects were Caucasian, one was Hispanic, and one was of Middle-Eastern origin. Of the 39 subjects, 33 required spectacle correction, and 32 of these individuals reported wearing contact lenses. Sixteen subjects wore daily disposable soft lenses, 14 wore monthly disposable soft lenses, one wore RGP lenses, and one wore extended wear soft lenses. Contact lenses were discontinued an average of 7.9 ± 11.2 days prior to measurements being taken.

The optical and biometric data of the 39 study subjects are presented in Table 3. In this data only the horizontal visible iris diameter revealed a statistically significant difference between right and left eyes. The sagittal height measurements of both the right and left eyes at chords of 10.0, 12.8 and 15.0 mm are presented in Table 4.

3.1. Sagittal height at a 10.0 mm chord

At the 10.0 mm chord, the OCT measurements of the right eyes revealed the greatest average sagittal height in the inferior segment and the least sagittal height in the nasal segment. The left eyes had the greatest average sagittal height in the inferior segment and the least sagittal height in the inferior nasal segment.

Table 3
Biometric data of the anterior segment anatomical features.

Anatomical Feature	Cross Section	Right Eye	± SD	Left Eye	± SD	Shapiro-Wilk Normality Test Passed? (α = 0.05)	p-value (two-tailed) Right vs. Left Eye
Horizontal Visible Iris Diameter (mm)	Horizontal	11.92	0.44	11.81	0.47	Yes	0.0023
Vertical Visible Iris Diameter (mm)	Vertical	11.33	0.51	11.24	0.52	Yes	0.0236
Palpebral Aperture (mm)	Vertical	10.65	0.89	10.65	0.87	Yes	0.9792
Corneal Diameter (mm)	Horizontal	13.02	0.45	13.03	0.50	Yes	0.6274
	Vertical	13.46	0.50	13.42	0.49	Yes	0.1709
	Oblique SN to IT	13.15	0.45	13.14	0.47	Yes	0.6869
	Oblique ST to IN	13.17	0.49	13.12	0.48	Yes	0.1087
Scleral Spur to Scleral Spur (mm)	Horizontal	11.93	0.44	11.95	0.50	Yes	0.5893
	Vertical	12.38	0.49	12.34	0.50	Yes	0.1657
	Oblique SN to IT	12.10	0.43	12.09	0.45	Yes	0.6313
	Oblique ST to IN	12.10	0.49	12.05	0.47	Yes	0.0653
Limbal Zone (mm)	Horizontal	0.55	0.10	0.61	0.15	Yes	0.0102
	Vertical	1.06	0.20	1.09	0.20	RE Yes/LE No	0.4702
Central Corneal Thickness (μm)	Mean	532.4	35.96	535.1	38.56	Yes	0.0976
Anterior Chamber Depth (mm)	Mean	3.30	0.29	3.30	0.28	Yes	0.7161
Grand Seiko WAM-5500	M	−2.20	2.69	−2.12	3.09	Yes	0.5579
Autorefraction (D)[a]	J_0	−0.03	0.42	+0.08	0.41	RE Yes/LE No	0.0158
	J_{45}	−0.07	0.30	+0.04	0.34	RE No/LE No	0.0777
Medmont E300 Topographer	M	44.2	1.50	44.4	1.51	Yes	0.0751
Simulated	J_0	−0.31	0.38	−0.36	0.39	Yes	0.2163
Keratometry (D)[b]	J_{45}	+0.01	0.25	+0.00	0.32	No	0.4975

[a] Autorefraction results displayed in power vectors terms spherical equivalence (M), vertical Jackson-Cross-Cylinder (J_0) and oblique Jackson-Cross-Cylinder (J_{45}).
[b] Corneal topography results of the simulated Keratometric power displayed in power vectors terms.

Table 4
Sagittal height measured by the Visante OCT at three chord lengths in eight primary meridians.

Chord Length	Meridian	n	Right Eye Height (μm)	±SD	Left Eye Height (μm)	±SD	Shapiro-Wilk Normality Test Passed? (α = 0.05)	p-value (two-tailed) Right vs. Left Eyes
10.0 mm	Nasal	39	1719	78	1712	84	Yes	0.4282
	Temporal	39	1789	89	1783	97	Yes	0.4282
	Superior Nasal	39	1785	91	1756	68	Yes	0.0055
	Inferior Temporal	39	1780	103	1783	89	Yes	0.8328
	Superior	39	1794	78	1793	90	Yes	0.8773
	Inferior	39	1810	90	1835	84	Yes	0.0041
	Superior Temporal	39	1792	82	1817	88	Yes	0.0203
	Inferior Nasal	39	1729	75	1737	85	Yes	0.3791
12.8 mm	Nasal	39	2898	151	2896	171	RE Yes/LE No	0.7075
	Temporal	39	2905	154	2896	171	RE Yes/LE No	0.6382
	Superior Nasal	39	2943	176	2908	165	Yes	0.0031
	Inferior Temporal	39	2929	182	2913	157	Yes	0.1994
	Superior	39	2906	150	2917	150	RE Yes/LE No	0.2747
	Inferior	39	2903	150	2929	151	RE Yes/LE No	0.0204
	Superior Temporal	39	2893	143	2915	143	Yes	0.0377
	Inferior Nasal	39	2900	144	2923	144	Yes	0.4754
15 mm	Nasal	39	3708	211	3710	224	Yes	0.8818
	Temporal	39	3772	222	3787	237	Yes	0.2804
	Superior Nasal	38	3754	242	3727	225	Yes	0.0844
	Inferior Temporal	39	3794	250	3756	228	Yes	0.0071
	Superior	39	3767	201	3780	201	RE Yes/LE No	0.2878
	Inferior	39	3723	201	3754	203	Yes	0.0214
	Superior Temporal	39	3747	186	3763	179	Yes	0.2498
	Inferior Nasal	39	3676	199	3728	182	Yes	0.0004

3.2. Sagittal height at a 12.8 mm chord

At the 12.8 mm chord, the OCT measurements of the right eyes revealed the greatest average sagittal height in the superior nasal segment and the least sagittal height in the superior temporal segment. The left eyes had the greatest average sagittal height in the inferior segment and the least sagittal height in the nasal and temporal segments.

3.3. Sagittal height at a 15.0 mm chord

At the 15.0 mm chord, the OCT measurements of the right eyes revealed the greatest average sagittal height in the inferior temporal segment and the least sagittal height in the inferior nasal segment. The left eyes had the greatest average sagittal height in the temporal segment and the least sagittal height in the nasal segment. A statistically significant difference between the scleral sagittal height measurements of right and left eyes was found in the inferior nasal segment.

In Table 5, the difference in sagittal height of the two opposing meridians in each cross-section are displayed to show the asymmetry of the sclera across each section.

To classify scleral toricity orientation, each eye was categorized into one of the following groups: with-the-rule (WTR), against-the-rule (ATR), oblique with the flat meridian at 45°, oblique with the flat meridian at 135°, or no toricity. The greatest height difference between two perpendicular meridians was defined as the scleral toricity. The flat meridian was defined as the meridian with the lowest sagittal height (Table 6). There did not appear to be a strong association between the orientation of the corneal astigmatism and the orientation of the scleral toricity in this normal population with low corneal astigmatism (OD 0.93 ± 0.59D; OS 1.00 ± 0.73D). Only 11 right eyes (28%) and 14 left eyes (38%) revealed an association between the corneal and scleral toricity. In these associated right eyes the mean scleral toricity at the 15.0 mm chord was 206 ± 41 μm, in the left eyes it was 199 ± 115 μm.

3.4. Scleral angles

The scleral angles at the 12.8 and 15.0 mm chords in each of the eight segments are presented in Table 7. A significant difference between right and left eyes in measured angles was identified only in the inferior nasal meridian at a 15.0 mm chord.

3.5. Corneoscleral junction angles

The CSJ angles at a fixed chord of 12.8 mm are shown in Table 8. Fig. 5 illustrates the relative frequency distribution of CSJ angles among all right eyes and left eyes in the four primary meridians. In both right and left eyes the nasal quadrant presented with a concave cornea to sclera transition on average, whereas all other quadrants were more tangential.

4. Discussion

Previous studies are in agreement regarding the mean scleral sagittal depth at a chord of 15.0 mm, along both the horizontal and vertical sagittal cross-sections [5–8] (Table 1). In addition, the corneoscleral junction angles have been reported in two studies [6,7]. The results of this study revealed lesser degree CSJ angles than previous studies, however were in agreement that the nasal quadrant has the lowest angle and is more concave in transition. It has been proposed that the shape of the nasal sclera is due to the relative anterior insertion of the medial rectus muscle [6,13,35], which inserts closer to the limbus than all other extraocular muscles [36–38]. The measured dimensions of the anterior eye (corneal diameter, corneal curvature, ACD, etc.) in this study are consistent with previously published data.

4.1. 10.0 mm chord

At a chord length of 10.0 mm, measurements of corneal shape using anterior segment OCT and corneal topography were not able to be directly compared due to the difference in measurement strategies and eye alignment techniques between the two instruments. The OCT measurements at this chord length revealed a significant difference in sagittal height between the segment with the greatest height and the segment with the least height (right eyes 91 μm, left eyes 98 μm). The pattern was such that the least sagittal depth occurred approximately along the horizontal meridian, and the greatest sagittal depth along the

Table 5
Sagittal height difference between opposing meridians at three chord lengths.

Chord Length	Cross Sections Compared	n	Right Eye: Height Difference Between Opposing Meridians[a] (μm)	Right Eye: p-value (two-tailed)	Left Eye: Height Difference Between Opposing Meridians[a] (μm)	Left Eye: p-value (two-tailed)
10.0 mm	Nasal – Temporal	39	−70	< 0.0001	−70	< 0.0001
	Superior – Inferior	39	−20	0.1865	−50	< 0.0001
	Superior Nasal – Inferior Temporal	39	+10	0.6794	−20	0.0069
	Superior Temporal – Inferior Nasal	39	+60	< 0.0001	+80	< 0.0001
12.8 mm	Nasal – Temporal	39	−10	0.1140	0	0.7369
	Superior – Inferior	39	+10	0.9194	−10	0.0168
	Superior Nasal – Inferior Temporal	39	+10	0.0131	0	0.3597
	Superior Temporal – Inferior Nasal	39	−10	0.1007	0	0.1052
15.0 mm	Nasal – Temporal	39	−60	< 0.0001	−80	< 0.0001
	Superior – Inferior	39	+50	< 0.0001	+30	0.0021
	Superior Nasal – Inferior Temporal	38	−40	0.0019	−30	0.0005
	Superior Temporal – Inferior Nasal	39	+70	< 0.0001	+30	< 0.0001

[a] The sagittal height difference between the opposing meridians is shown, with a positive value (+) indicating that the first meridian listed has the higher sagittal height; a negative value (−) indicates that the first meridian has the lower sagittal height.

Table 6
Scleral Toricity at a 15.0 mm chord classified by orientation.

Scleral Toricity Orientation	# Subjects	**Mean Scleral Toricity**[a] Right Eye	# Subjects	**Mean Scleral Toricity**[a] Left Eye
With-the-Rule	10	170 μm	10	190 μm
Against-the-Rule	12	130 μm	14	140 μm
Oblique: Flat meridian ~ 45°	2	80 μm	5	130 μm
Oblique: Flat Meridian ~ 135°	14	170 μm	8	140 μm
No Toricity	0	–	2	0 μm

[a] Scleral toricity was defined as the greatest sagittal height difference found between two perpendicular meridians.

vertical meridian, corresponding to with-the-rule corneal astigmatism.

4.2. 12.8 mm chord

Compared to the 10.0 mm chord, the 12.8 mm chord data showed a significantly smaller difference between the segments with the greatest and least sagittal heights (right eyes 50 μm, left eyes 33 μm). These data appear to indicate that at the 12.8 mm chord, the eye is more rotationally symmetric than at the 10.0 mm chord.

4.3. 15.0 mm chord

At the 15.0 mm chord, the sclera was found to be significantly more asymmetric (maximum vs. minimum sagittal height differential of 118 μm in right eyes, 77 μm in left eyes) than at the 12.8 mm chord, particularly when comparing nasal to temporal shape, but less so than other studies have suggested [6,7]. The general scleral shape discovered was rotationally asymmetric with a flatter nasal hemisphere than temporal.

These data indicate that on average the eye demonstrates with-the-rule corneal astigmatism, apparent at the 10.0 mm chord. This transitions to a more symmetrical surface at the 12.8 mm chord, and at the 15.0 mm chord, the sclera takes on a more rotationally asymmetric shape. These results suggest that adding toricity or asymmetry to the periphery of a scleral lens in order to achieve an optimal fit is likely more critical with larger diameter lenses compared to smaller diameter lenses.

Table 7
Ocular angle measurements in eight primary meridians.

Chord Length	Meridian	n	Right Eye Angle (Degrees)	±SD	Left Eye Angle (Degrees)	±SD	Shapiro-Wilk Normality Test Passed? ($\alpha = 0.05$)	p-value (two-tailed) Right vs. Left Eyes
12.8 mm	Nasal	39	39.85	2.29	40.14	2.67	RE Yes/LE No	0.0446
	Temporal	39	38.53	1.95	38.42	2.50	RE Yes/LE No	0.9752
	Superior Nasal	39	39.36	2.96	39.38	3.01	Yes	0.9479
	Inferior Temporal	39	39.32	2.60	38.78	2.29	Yes	0.0112
	Superior	39	38.35	2.50	38.69	2.37	Yes	0.0695
	Inferior	39	37.98	2.33	37.79	2.37	Yes	0.2717
	Superior Temporal	39	38.15	2.40	38.10	2.21	Yes	0.7607
	Inferior Nasal	39	39.66	2.47	40.18	2.63	RE Yes/LE No	0.0092
15.0 mm	Nasal	39	36.36	3.00	36.46	2.76	Yes	0.6923
	Temporal	39	38.17	2.64	38.82	2.70	Yes	0.0007
	Superior Nasal	38	36.22	2.66	36.55	2.57	Yes	0.3000
	Inferior Temporal	39	37.99	2.82	37.34	2.70	Yes	0.0196
	Superior	39	38.01	2.47	37.93	2.27	Yes	0.6911
	Inferior	39	36.70	2.56	36.72	2.57	Yes	0.9320
	Superior Temporal	39	37.70	1.96	37.55	1.77	Yes	0.4633
	Inferior Nasal	39	35.17	2.26	36.26	2.28	Yes	< 0.0001

Table 8
Corneoscleral junction angle (CSJ) measurements at the 12.8 mm chord.

Meridian	n	Right Eye Angle (Degrees)	± SD	Left Eye Angle (Degrees)	± SD	Shapiro-Wilk Normality Test Passed? (α = 0.05)	p-value (two-tailed) Right vs. Left Eyes
Nasal	39	176.50	2.47	176.30	2.39	Yes	0.4498
Temporal	39	179.60	1.81	180.40	1.49	Yes	0.0054
Superior Nasal	38	176.80	1.95	177.20	2.07	Yes	0.3672
Inferior Temporal	39	178.70	1.72	178.60	1.70	Yes	0.6783
Superior	39	179.70	1.95	179.20	1.88	Yes	0.1478
Inferior	39	178.70	2.03	178.90	2.01	Yes	0.4566
Superior Temporal	39	179.50	1.99	179.50	1.74	Yes	0.7145
Inferior Nasal	39	175.50	1.55	176.10	2.15	Yes	0.0339

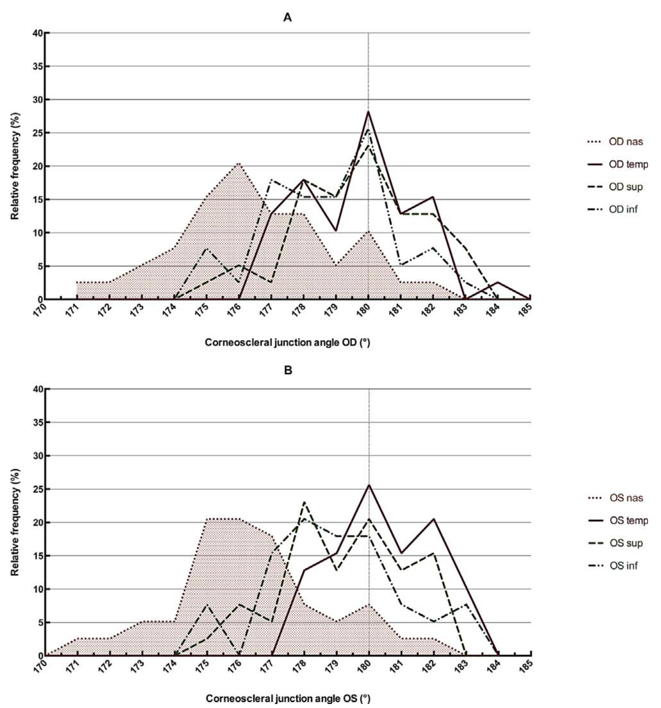

Fig. 5. Relative frequency distribution of the corneoscleral junction angle measurements at chord length of 12.8 mm; the shaded area represents the segment in which measurements deviated most from the average of all segments A) all four primary quadrants of the right eyes (OD) B) all four primary quadrants of the left eyes (OS).

4.4. Scleral angles

At the 12.8 mm chord, the corneoscleral angles were largest (highest) in the three nasal segments (superior nasal, nasal, and inferior nasal). At the 15.0 mm chord, these three nasal angles were the smallest (lowest). This suggests that the transition from cornea to sclera is fairly abrupt and is more concave in the nasal segments. At the 12.8 mm chord, the angles were smallest in the three temporal segments (superior temporal, temporal, and inferior temporal), and at the 15.0 mm chord, these temporal angles were largest. This indicates a more convex corneoscleral shape temporally. The difference in angle measurements temporally between the 12.8 and 15.0 mm chords was minimal (right eyes 0.36°, left eyes 0.40°). The difference in angle measurements nasally between the 12.8 and 15.0 mm chords was more significant (right eyes 3.49°, left eyes 3.68°). This indicates a more tangent-like profile of the temporal sclera as compared to the nasal sclera.

Therefore, on the Visante OCT images the corneoscleral sulcus is expected to be more distinct and easily identifiable in the three nasal segments than in the three temporal segments where there was a smooth tangential transition. A more accurate method of identifying the corneoscleral junction consistently across all segments is the technique described earlier in this study (Fig. 3). These findings imply that slit lamp biomicroscopy classification of the corneoscleral transition profiles (CSP) [39,40] of any given segment cannot be used to derive specific information about the other segments.

4.5. Contact lens positioning properties

Based on these data, the shape of the anterior eye will affect the centration properties of a spherical scleral lens in the following manner: the lens will land first on the segment of the eye with the least sagittal height (greatest elevation), and then move in the direction of least mechanical resistance, toward the segment with the greatest sagittal height (lowest elevation). Gravity and eyelid forces may also act on the lens, contributing to some degree of inferior decentration. An inferior-temporal decentration is therefore to be expected in most scleral contact lenses.

4.6. Scleral toricity

Average scleral toricity (defined as the greatest sagittal height difference found between two perpendicular meridians) at a 15.0 mm chord was 150 ± 77 µm in right eyes and 159 ± 85 µm in left eyes. This indicates that for scleral lenses that land at chords of 15.0 mm or greater, a toric haptic may be beneficial. The use of toric haptic designs is also supported by Visser et al. [41] and serves to provide increased comfort and a more aligned fit on the sclera. The use of toric haptics can also serve as an orientation mechanism for rotational stability of scleral lenses. This can assist in properly aligning optics over the pupil in lenses with cylinder correction, multifocal optics, and higher order aberration corrections [42,43].

There was not a significant association between the orientation of corneal astigmatism and scleral astigmatism in this normal population. In the right eye, of 11 subjects that had corneal astigmatism between 1.00 and 2.00D, only three eyes (27%) revealed the same orientation of the scleral and corneal astigmatism. Higher corneal astigmatism (> 2.00D) appeared to be more associated with scleral toricity. A more detailed investigation of the association between corneal and scleral toricity is necessary in eyes with corneal astigmatism greater 2.00D.

4.7. Potential factors influencing scleral shape

There are several factors that presumably influence the shape of the anterior sclera, including extraocular muscle anatomy. A possible contributor to scleral shape is the orientation of extraocular rectus muscle insertions [6,13,35]. The proximity of two adjacent extraocular muscles may also contribute to the shape of the sclera. The medial and inferior rectus muscles have the shortest distance between their insertions [36]. This close proximity of adjacent muscles may create a flatter contour of the eye at a chord of 15.0 mm, whereas the greater distance between the inferior and lateral rectus muscles may contribute to a steeper temporal scleral shape (Fig. 6).

Age is another factor that can affect the shape of the sclera. This variable was not addressed in this particular study. With aging, the

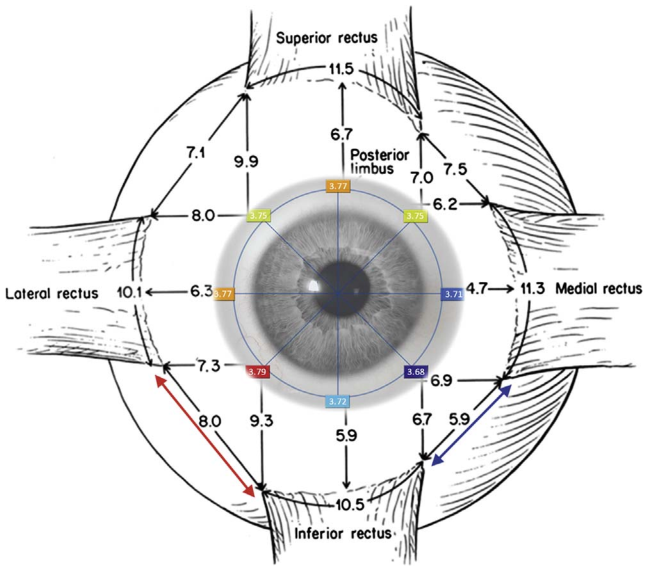

Fig. 6. Superimposed image of the average sagittal height of right eyes of the present study on Apt's muscle insertion figure; the blue arrow marks the shortest distance between adjacent muscles, the red arrow marks the longest distance.

corneal curvature becomes steeper [44], HVID and VVID smaller [32], and anterior chamber width and depth narrower and shallower [44–46]. Therefore, external scleral angles and sagittal heights may also change with age, although further studies are required to confirm this.

Eyelid forces and lid position (angle of lid inclination) have been shown to affect corneal shape and curvature [47–51]. Their effect on scleral shape is unknown at this time.

Another factor potentially influencing the shape of the anterior sclera is axial length. Hosny et al. [52] investigated several ocular variables and organized them in relation to axial length. With increasing axial length, a corresponding increase was found in corneal diameter, anterior chamber depth, and myopic refractive error. This suggests that axial length may influence anterior segment sagittal depth and scleral shape.

4.8. Variation of HVID, VVID, corneal diameter and limbal zone

The posterior corneal diameter was measured between opposing sides of the scleral spur. Both corneal diameter and scleral spur to scleral spur distance were longer vertically than horizontally, which is consistent with previous studies [46,53,54]. In contrast, the HVID was found to be longer than the VVID on average in this study and in previous studies [6,7,30,32]. This implied a discrepancy between the widths of the limbal zones (LZ) horizontally and vertically. In clinical observation and in the literature, [30,36] the superior LZ is wider than the inferior LZ.

4.9. Study limitations

The primary limitations of this study were related to measurement acquisition and quality using the Visante OCT. The most notable limitation of the instrument was the optical axial resolution of 18 μm and caliper accuracy of 10 μm. Additionally, the placement of the anterior chamber tool to measure the sagittal height and scleral angles involved some subjectivity, which could be subject to bias and human error.

The scanning speed of 2000 (A-scans/s) could be considered a limiting factor in measuring accuracy and micro eye movements with the Anterior Segment Quadscan mode. The scanning width of 16.0 mm was another limiting factor, as no scleral shape data could be acquired beyond 16.0 mm. Other investigators have addressed this limitation by stitching multiple images together [13,27,28], which may be a source for additional error.

Today, new anterior segment imaging technologies have emerged, some are capable of measuring the sclera 360° around. The Zeiss Cirrus HD OCT measures up to a 15.5 mm chord length, yet with only one cross-section per scan. Modern profilometry instruments such as the Eye Surface Profiler (Eaglet Eye) and the sMap3D (Precision Ocular Metrology) can measure scleral shape up to a 20.0 mm chord.

5. Conclusion

This study provides new insights into the shape of the anterior sclera by measuring the sagittal height and ocular angles across eight radial segments.

The results of this study indicate that in the limbal area, at a chord of 12.8 mm, the average shape of the eye is nearly rotationally symmetric, as it shows only very small differences in sagittal height between opposing segments. The shape of the sclera at a chord of 15.0 mm becomes more rotationally asymmetric. For scleral lens fitting purposes, the scleral asymmetry was interpreted as toricity, which was defined as the greatest sagittal height difference found between two perpendicular meridians. The average amount of toricity found in this study indicates that a toric haptic may improve lens alignment for lenses that land at a chord of 15.0 mm or greater.

A consistent pattern has been revealed in both corneoscleral and scleral angles. The corneoscleral angles at 12.8 mm are steeper in the nasal hemisphere than in the temporal. In contrast, the scleral angles at 15.0 mm in the nasal hemisphere are flatter than in the temporal. It appears that the corneoscleral junction angle in the nasal hemisphere shows an abrupt, concave transition. In the temporal hemisphere a more convex and tangential transition occurs.

In regards to lens centration, the results of this study suggest that scleral lenses will decenter temporally and inferiorly. This is due to the fact that a scleral lens lands first on the most elevated nasal segment and is expected to settle and move toward the opposing, less elevated segment as it finds its equilibrium. In addition, the nasal segment will likely have less clearance between the lens and the cornea due to the corneoscleral angle being larger and scleral angle being smaller than the temporal.

Scleral shape, gravity, and eyelid forces during blinking all may contribute to the inferior temporal decentration found with most scleral lenses. Proper landing zone alignment in each scleral segment may help support an optimally centered lens. Based on the findings of this study, complex geometries such as toric or segment specific peripheral designs are likely required to achieve this in many eyes.

Today, diagnostic scleral lenses are evaluated on-eye to determine the optimum lens parameters required. Instruments designed to aid this process should measure scleral shape efficiently and accurately in order to serve an application in clinical contact lens practice. In the future, perhaps the knowledge gained through this study, along with advancements in technology, may further improve the process of scleral lens fitting.

References

[1] E.S. Bennett, B.A. Weissman, Clinical contact sens practice, Lippincott Williams & Wilkins, 2005.
[2] G. Gemoules, A novel method of fitting scleral lenses using high resolution optical coherence tomography, Eye Contact Lens Sci Clin Pract 34 (2008) 80–83.
[3] E. van der Worp, A guide to scleral lens fitting [cited 2014 Jul 26], (2010) Available from: http://commons.pacificu.edu/mono/4/.
[4] M.M. Schornack, S.V. Patel, Relationship between corneal topographic indices and scleral lens base curve, Eye Contact Lens 36 (2010) 330–333.
[5] L. Sorbara, J. Maram, D. Fonn, C. Woods, T. Simpson, Metrics of the normal cornea: anterior segment imaging with the Visante OCT: metrics of the normal cornea, Clin Exp Optom 93 (2010) 150–156.
[6] L.A. Hall, G. Young, J.S. Wolffsohn, C. Riley, The influence of corneoscleral topography on soft contact lens fit, Invest Ophthalmol Vis Sci 52 (2011) 6801–6806.
[7] L.A. Hall, C. Hunt, G. Young, J. Wolffsohn, Factors affecting corneoscleral topography, Invest Ophthalmol Vis Sci 54 (2013) 3691–3701.

[8] L. Sorbara, J. Maram, K. Mueller, Use of the Visante™ OCT to measure the sagittal depth and scleral shape of keratoconus compared to normal corneae: pilot study, J Optom 6 (2013) 141–146.
[9] B. Baldwin, S. Moyer, AS-OCT and the specialty contact lens. Rev cornea contact lenses [cited 2017 Jun 8], (2012) Available from http://www.reviewofcontactlenses.com/content/c/33645/.
[10] P.J. Caroline, M.P. André, Scleral lenses do not center, Contact Lens Spectr 29 (2014) 56.
[11] H.-G.T. Le, M. Tang, R. Ridges, D. Huang, D.S. Jacobs, Pilot study for OCT guided design and fit of a prosthetic device for treatment of corneal disease, J Ophthalmol 2012 (2012) 1–7.
[12] R. Kojima, P.J. Caroline, T. Graf, B. Kinoshita, L. Copilevitz, R. Achong-Coan, et al., Eye shape and scleral lenses, Contact Lens Spectr 3 (2013) 8–43.
[13] H.J. Choi, S.-M. Lee, J.Y. Lee, S.Y. Lee, M.K. Kim, W.R. Wee, Measurement of anterior scleral curvature using anterior segment OCT, Optom Vis Sci Off Publ Am Acad Optom 91 (2014) 793–802.
[14] D. Ezekiel, Gas permeable haptic lenses, J Br Contact Lens Assoc 6 (1983) 158–161.
[15] N. Efron, Contact lens practice, Elsevier Health Sciences, 2010.
[16] E. van der Worp, D. Bornman, D.L. Ferreira, M. Faria-Ribeiro, N. Garcia-Porta, J.M. González-Meijome, Modern scleral contact lenses: a review, Contact Lens Anterior Eye 37 (2014) 240–250.
[17] M.M. Schornack, Scleral lenses: a literature review, Eye Contact Lens Sci Clin Pract 41 (2015) 3–11.
[18] V. Compañ, C. Oliveira, M. Aguilella-Arzo, S. Mollá, S.C. Peixoto-de-Matos, J.M. González-Méijome, Oxygen diffusion and edema with modern scleral rigid gas permeable contact lenses, Invest Ophthalmol Vis Sci 55 (2014) 6421–6429.
[19] T. Romero-Rangel, P. Stavrou, J. Cotter, P. Rosenthal, S. Baltatzis, C.S. Foster, Gas-permeable scleral contact lens therapy in ocular surface disease, Am J Ophthalmol 130 (2000) 25–32.
[20] P. Rosenthal, J.M. Cotter, J. Baum, Treatment of persistent corneal epithelial defect with extended wear of a fluid-ventilated gas-permeable scleral contact lens, Am J Ophthalmol 130 (2000) 33–41.
[21] P. Rosenthal, A. Croteau, Fluid-ventilated, gas-permeable scleral contact lens is an effective option for managing severe ocular surface disease and many corneal disorders that would otherwise require penetrating keratoplasty, Eye Contact Lens 31 (2005) 130–134.
[22] B. Severinsky, M. Millodot, Current applications and efficacy of scleral contact lenses—a retrospective study, J Optom 3 (2010) 158–163.
[23] M.M. Schornack, S.V. Patel, Scleral lenses in the management of keratoconus, Eye Contact Lens Sci Clin Pract 36 (2010) 39–44.
[24] E. van der Worp, Scleral lens case report series: beyond the corneal borders [cited 2014 Jul 26], (2012) Available from http://commons.pacificu.edu/mono/5/.
[25] S.L.P. Weber, R.B. de Souza, J.Á.P. Gomes, A.L. Hofling-Lima, The use of the esclera scleral contact lens in the treatment of moderate to severe dry eye disease, Am J Ophthalmol 163 (2016) 167–173 e1.
[26] V. Rathi, M. Taneja, P. Mandathara, V. Sangwan, S. Dumpati, Scleral lens for keratoconus: technology update, Clin Ophthalmol (2015) 2013.
[27] S.-M. Lee, H.J. Choi, H. Choi, M.K. Kim, W.R. Wee, Estimation of axial curvature of anterior sclera: correlation between axial length and anterior scleral curvature as affected by angle kappa, BMC Ophthalmol 16 (2016), http://dx.doi.org/10.1186/s12886-016-0355-5.
[28] E. van der Worp, T. Graf, P.J. Caroline, Exploring beyond the corneal borders, Contact Lens Spectr 6 (2010) 26–32.
[29] W. Eugene, Eugene Wolff's Anatomy of the eye and orbit: including the central connexions, development, and comparative anatomy of the visual apparatus, 7th ed., Saunders, Philadelphia, 1976 /rev. by Roger Warwick.
[30] E.M. Van Buskirk, The anatomy of the limbus, Eye (1989) 101–108.
[31] F. Rüfer, A. Schröder, C. Erb, White-to-white corneal diameter: normal values in healthy humans obtained with the Orbscan II topography system, Cornea 24 (2005) 259–261.
[32] E. Iyamu, E. Osuobeni, Age, gender, corneal diameter, corneal curvature and central corneal thickness in Nigerians with normal intra ocular pressure, J Optom 5 (2012) 87–97.
[33] M.J. Hogan, J.A. Alvarado, J.E. Weddell, Histology of the human eye: an atlas and textbook [by] Michael J. Hogan, Jorge A. Alvarado [and] Joan Esperson Weddell. Saunders, (1971).
[34] W.A. Ray, D.M. O'day, Statistical analysis of multi-eye data in ophthalmic research, Invest Ophthalmol Vis Sci 26 (1985) 1186–1188.
[35] P.J. Marriott, An analysis of the global contours and haptic contact lens fitting, Br J Physiol Opt 23 (1966) 1–40.
[36] L. Apt, An anatomical reevaluation of rectus muscle insertions, Trans Am Ophthalmol Soc 78 (1980) 365.
[37] E.E. Villarreal-Silva, J.M. Hinojosa Amaya, J.J. Bazaldua Cruz, D. Martínez Fernández, R.E. Elizondo-Omaña, S. Guzmán López, A morphometric study of the extraocular muscles, Int J Morphol 31 (2013) 312–320.
[38] S. Mukhopadhyay, S. Chakraborty, M. Chatterjee, H. Datta, A study on the insertion characteristics of the rectus muscles and its relation with the axial lengh of the eyebal in cadaveric eyes from an eastern indian population, Anat J Afr 3 (2014) 26–267.
[39] D. Meier, Das Cornea-Skleral-Profil – ein Kriterium individueller Kontaktlinsenanpassung, Kontaktlinse 26 (1992) 4–11.
[40] S. Bokern, M. Hoppe, S. Bandlitz, Genauigkeit und wiederholbarkeit bei der klassifizierung des corneoskleral profils, Kontaktlinse (2007) 7–8.
[41] E.S. Visser, R. Visser, H.J. Van Lier, Advantages of toric scleral lenses, Optom Vis Sci 83 (2006) 233–236.
[42] R. Sabesan, L. Johns, O. Tomashevskaya, D.S. Jacobs, P. Rosenthal, G. Yoon, Wavefront-guided scleral lens prosthetic device for keratoconus, Optom Vis Sci 90 (2013) 314–323.
[43] J.D. Marsack, A. Ravikumar, C. Nguyen, A. Ticak, D.E. Koenig, J.D. Elswick, et al., Wavefront-guided scleral lens correction in keratoconus, Optom Vis Sci 91 (2014) 1221–1230.
[44] K. Hayashi, H. Hayashi, F. Hayashi, Topographic analysis of the changes in corneal shape due to aging, Cornea 14 (1995) 527–532.
[45] D.G. Lee, S.H. Choi, Measurement of anterior segment using Visante OCT in Koreans, J Korean Ophthalmol Soc 50 (2009) 542.
[46] B. Qin, X. Zhou, D. Huang, R. Chu, Effects of age on ocular anterior segment dimensions measured by optical coherence tomography, Chin Med J-Beijing 124 (2011) 1829.
[47] S.A. Read, M.J. Collins, L.G. Carney, The influence of eyelid morphology on normal corneal shape, Invest Ophthalmol Vis Sci 48 (2007) 112–119.
[48] S.A. Read, The topography of the central and peripheral cornea, Invest Ophthalmol Vis Sci 47 (2006) 1404–1415.
[49] S.A. Read, Corneal topography and the morphology of the palpebralfissure [cited 2015 Jul 7], (2006) Available from http://eprints.qut.edu.au/16203/.
[50] G. Wilson, C. Bell, S. Chotai, The effect of lifting the lids on corneal astigmatism, Am J Optom Physiol Opt 59 (1982) 670–674.
[51] C. Grey, M. Yap, Influence of lid position on astigmatism, Optom Vis Sci 63 (1986) 966–969.
[52] M. Hosny, J.L. Alio, P. Claramonte, W.H. Attia, J.J. Pérez-Santonja, Relationship between anterior chamber depth, refractive state, corneal diameter, and axial length, J Refract Surg 16 (2000) 336–340.
[53] G. Baikoff, H. Jitsuo Jodai, G. Bourgeon, Measurement of the internal diameter and depth of the anterior chamber: iOLMaster versus anterior chamber optical coherence tomographer, J Cataract Refract Surg 31 (2005) 1722–1728.
[54] P.-S. Yan, H.-T. Lin, Q.-L. Wang, Z.-P. Zhang, Anterior segment variations with age and accommodation demonstrated by slit-lamp-adapted optical coherence tomography, Ophthalmology 117 (2010) 2301–2307.